Observation and Astrometric Study of Double Star Systems HJ 824, COO 273, LEO 57, and UC 89

Ava Angeles[1], Roshan Bellary[1], Zongshu Wu[1], Raka Bose[1], Kalée Tock[1]
[1]Stanford Online High School, Redwood City, CA 94063; angeles8@ohs.stanford.edu

Abstract: This study presents measurements of the double star systems WDS 09576+0910 (HJ 824), WDS 00002-2519 (COO 273), WDS 05267+0045 (LEO 57), and WDS 06272+1933 (UC 89) and investigates whether each of the star systems are gravitationally bound and/or have common proper motion. After requesting images from the Las Cumbres Observatory (LCOGT), images of each system were reduced using AstroImageJ (AIJ) to determine the position angle and separation of the secondary stars from their corresponding primaries. Historical plots were made based on previous measurements as well as the measurements taken in this study. In addition, an analysis of the likelihood of gravitational bondage was done by setting the stars' relative velocity equal to escape velocity and calculating maximum spatial separation. Using the relative proper motion metric developed by Richard Harshaw, an analysis of the stars' proper motion was also made. All three of these methods were used to evaluate the likelihood that the secondary star in each star system was gravitationally bound to the primary star. The evidence suggests that the stars in HJ 824, COO273, and UC 89 are not gravitationally bound but are moving together in space with common proper motion, while LEO 57 is likely to be a gravitationally bound pair.

1. Introduction

HJ 824 is a double star system located at RA 09 57 35.12 and Dec +09 09 38.4 in the constellation Leo; LEO 57 is located in the constellation Orion and has coordinates of RA 05 26 39.67 and Dec +00 45 02.2. COO 273 has coordinates of RA 00 00 09.71 and Dec -25 19 29.3, and UC 89 has coordinates of RA 06 27 09.33 and Dec +19 32 53.2. These systems were chosen as they were visible in the night sky at the time of this study, and the systems were previously classified to be physical. Also, the magnitudes of the secondary stars were less than 13 in order for both the primary and secondary to be visible in images. Additionally, the differences in magnitudes between the two stars were less than 3, since similarity in brightness allows both stars to be clearly resolved using the same exposure time. Lastly, the separation between the stars was constrained to be between 5 and 20 arcseconds, as stars too close together would be difficult to separate, and stars too far apart are less likely to share a physical connection.

2. Equipment and Methods

The images used in this study were taken by 0.4m diameter robotic telescopes from the Las Cumbres Observatory Global Telescope (LCOGT) network equipped with charge-coupled device (CCD) cameras. These telescopes are equipped with many filters, including the panSTARRS-W filters used in this study. HJ 824 and UC 89 were imaged in Tenerife Observatory in the Canary Islands, while COO 273 was imaged in Cerro Tololo Observatory in Chile, and LEO 57 was imaged in Siding Spring Observatory in Australia.

Using AstroImageJ software, a series of 10 images for each star was taken by the LCOGT telescopes and reduced to determine the position angle (PA) and separation (Sep) of each double star system. AstroImageJ allows the user to find the centroid of the star automatically using the position that represents the weighted average of the pixel brightnesses within a chosen aperture. A viable aperture size is sufficiently large to enclose the star, but not so large that the apertures of the two stars overlap. In addition, the exposure time chosen for each image must be long enough to capture each star, but not so long that the telescope's lens gets oversaturated. Following these parameters, the chosen aperture sizes and the exposure times for each system's images are in the table below.

Table 1: Aperture size and exposure times for each system.

System	**Aperture Size (Pixels)**	**Exposure Time (seconds)**
HJ 824	8	30
COO 273	4	20
LEO 57	7	15
UC 89	8	19.5

After selecting an aperture size and zooming into the region of the image where the stars are located, the user command-drags the cursor from the primary to the secondary star to obtain the PA and Sep (shown as ArcLen). An example is shown for each star pair in Figs. 1-4.

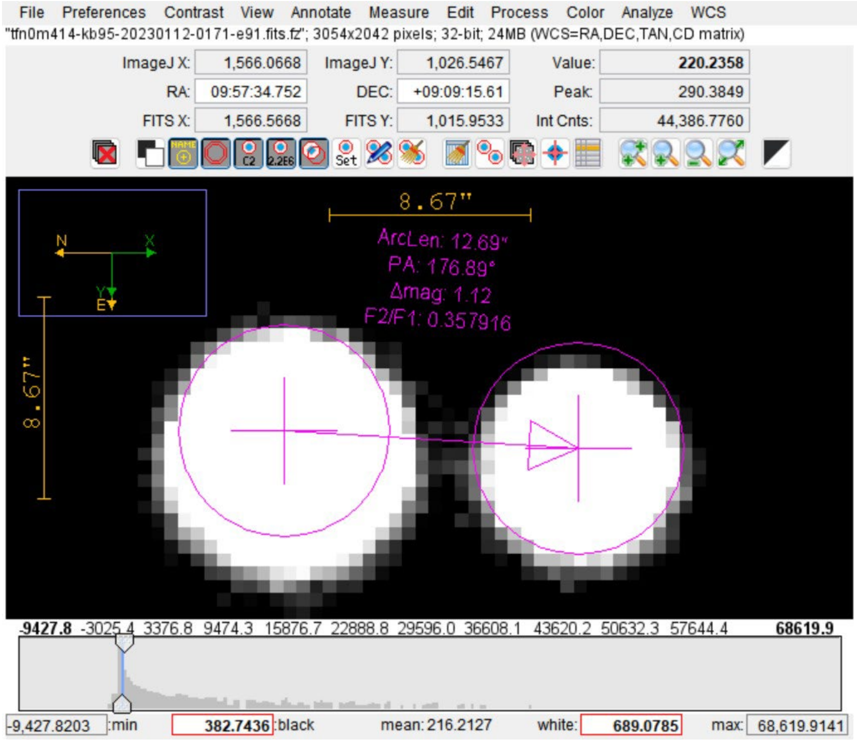

"tfn0m414-kb95-20230112-0171-e91.fits.fz"; 3054x2042 pixels; 32-bit; 24MB (WCS=RA,DEC,TAN,CD matrix)

ImageJ X: 1,566.0668 ImageJ Y: 1,026.5467 Value: 220.2358

RA: 09:57:34.752 DEC: +09:09:15.61 Peak: 290.3849

FITS X: 1,566.5668 FITS Y: 1,015.9533 Int Cnts: 44,386.7760

ArcLen: 12.69"
PA: 176.89°
Δmag: 1.12
F2/F1: 0.357916

-9,427.8203 :min 382.7436 :black mean: 216.2127 white: 689.0785 max: 68,619.9141

Figure 1: AIJ sample measurement of HJ 824.

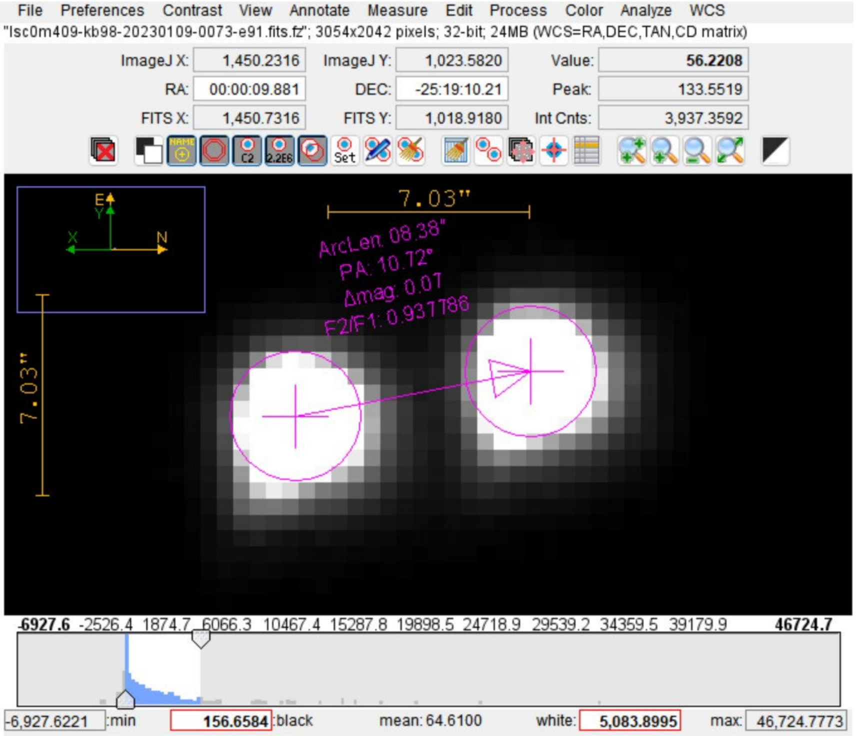

"lsc0m409-kb98-20230109-0073-e91.fits.fz"; 3054x2042 pixels; 32-bit; 24MB (WCS=RA,DEC,TAN,CD matrix)

ImageJ X: 1,450.2316 ImageJ Y: 1,023.5820 Value: 56.2208
RA: 00:00:09.881 DEC: -25:19:10.21 Peak: 133.5519
FITS X: 1,450.7316 FITS Y: 1,018.9180 Int Cnts: 3,937.3592

-6,927.6221 :min 156.6584 :black mean: 64.6100 white: 5,083.8995 max: 46,724.7773

Figure 2: AIJ sample measurement of COO 273.

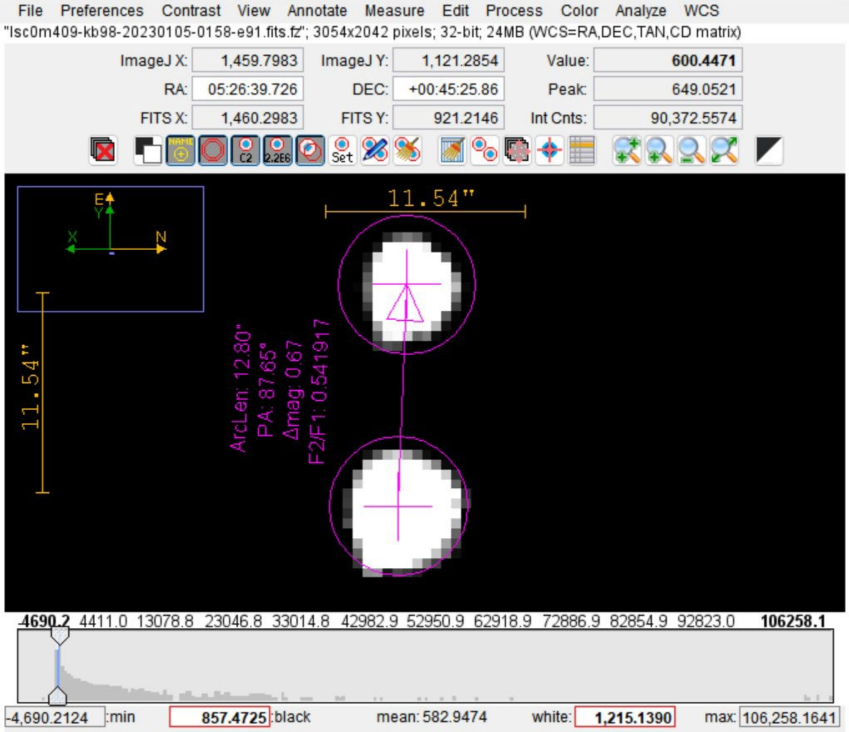

"lsc0m409-kb98-20230105-0158-e91.fits.fz"; 3054x2042 pixels; 32-bit; 24MB (WCS=RA,DEC,TAN,CD matrix)

ImageJ X: 1,459.7983 ImageJ Y: 1,121.2854 Value: 600.4471
RA: 05:26:39.726 DEC: +00:45:25.86 Peak: 649.0521
FITS X: 1,460.2983 FITS Y: 921.2146 Int Cnts: 90,372.5574

-4,690.2124 :min 857.4725 :black mean: 582.9474 white: 1,215.1390 max: 106,258.1641

Figure 3: AIJ sample measurement of LEO 57

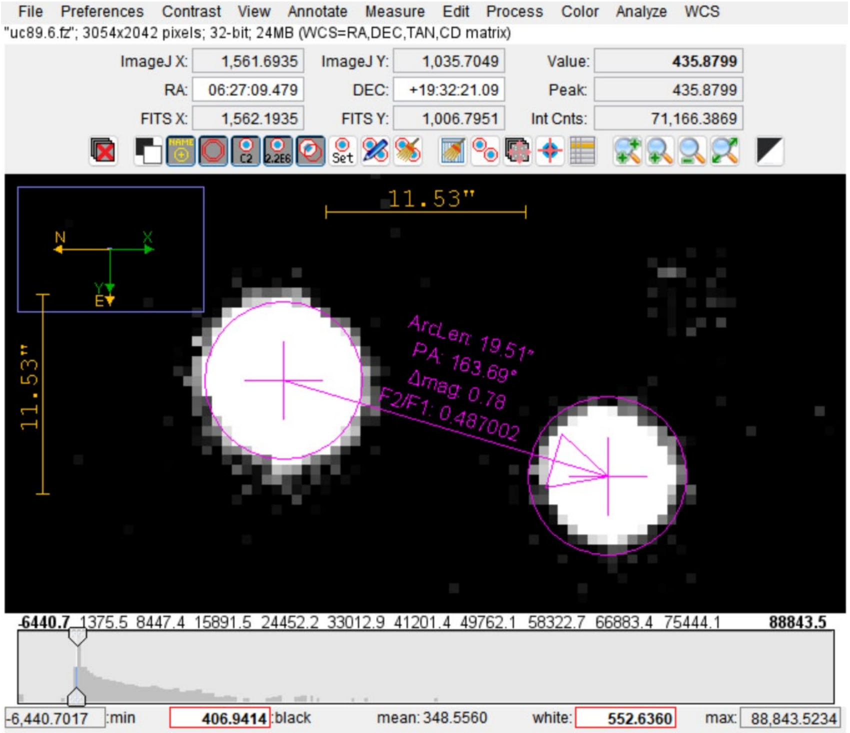

"uc89.6.fz"; 3054x2042 pixels; 32-bit; 24MB (WCS=RA,DEC,TAN,CD matrix)

ImageJ X: 1,561.6935 ImageJ Y: 1,035.7049 Value: 435.8799
RA: 06:27:09.479 DEC: +19:32:21.09 Peak: 435.8799
FITS X: 1,562.1935 FITS Y: 1,006.7951 Int Cnts: 71,166.3869

-6,440.7017 :min 406.9414 :black mean: 348.5560 white: 552.6360 max: 88,843.5234

Figure 4: AIJ sample measurement of UC 89.

In all images of LEO 57 and UC 89, the stars looked egg-shaped instead of symmetrical. This may be an indication that more stars are present in the system that have yet to be detected, or it may be the result of tracking irregularity or coma. The latter is more likely because both stars bulge in the same direction. However, this did not appear to have an adverse effect on the measurement, which is presented in the next section.

3. Data

From the measurement techniques presented in the previous section, we obtained the measurements presented in Table 2.

Table 2: Measurements taken from requested images.

System	Date	Number of Images	Position Angle (º)	Standard Error on PA (°)	Separation (″)	Standard Error* on Sep (″)
HJ 824	2023.0356	10	176.8	0.03	12.69	0.006
COO 273	2023.0274	10	10.7	0.04	8.41	0.014
LEO 57	2023.0164	10	87.7	0.02	12.82	0.008
UC 89	2023.0246	10	163.5	0.03	19.55	0.010

* The standard error is the “expected” deviation of the sample mean of the PA and Sep from the true value of the PA and Sep. In other words, if many samples of the same size were picked and the means calculated, the standard error would be an approximation of the standard deviation of those means.

Using data from the Gaia Data Release 3 (DR3), we calculated the proper motion of each star, as well as their rPM metric, which is used to compare their proper motions. These data are shown in Table 3.

Table 3: Parallax and Proper Motion data from the Gaia DR3 and the rPM metric.

System	**Parallax of Primary (mas)**	**Parallax of Secondary (mas)**	**PM of Primary in RA and Dec (mas/yr)**	**PM of Secondary in RA and Dec (mas/yr)**	**rPM**
HJ 824	4.45 ± 0.028	4.57 ± 0.034	-49.67, 35.97	-51.28, 37.85	0.039
COO 273	3.42 ± 0.016	3.39 ± 0.018	0.79, -8.39	1.07, -11.92	0.295
LEO 57	0.86 ± 0.014	0.83 ± 0.016	-0.18, -4.11	-0.22, -4.12	0.010
UC 89	4.23 ± 0.022	4.18 ± 0.017	29.09, -45.4	30.73, -45.54	0.030

The proper motion (PM) of a star, shown in columns 4 and 5 of Table 3, is its transverse velocity in RA and Dec across the sky. These numbers are used to calculate the relative velocity of the two stars. The rPM metric, formulated by Richard Harshaw, is the magnitude of the difference of the proper motions of the primary and secondary divided by the larger magnitude of the two proper motions (Harshaw, 2016). In other words, the rPM measures how different the two proper motions are from each other, relative to the size of the larger proper motion.

If the rPM of the stars is less than 0.2, then the stars are likely a Common Proper Motion (CPM) pair. Otherwise, if the rPM is less than 0.6, then the stars have Similar Proper Motion (SPM), and if the rPM is greater than 0.6, then they have Distinct Proper Motion (DPM). Therefore, the stars in COO 273 have Similar Proper Motion while the stars in the other three systems have Common Proper Motion.

Using historical data from the U.S. Naval Observatory, plots were made of the motion of these system's secondaries around their primaries. These plots, presented in Figs. 5-8 with the right ascension on the x-axis and the declination on the y-axis, display the data with this study's measurements marked in red. The green points on the plots represent the measurements acquired from Gaia data.

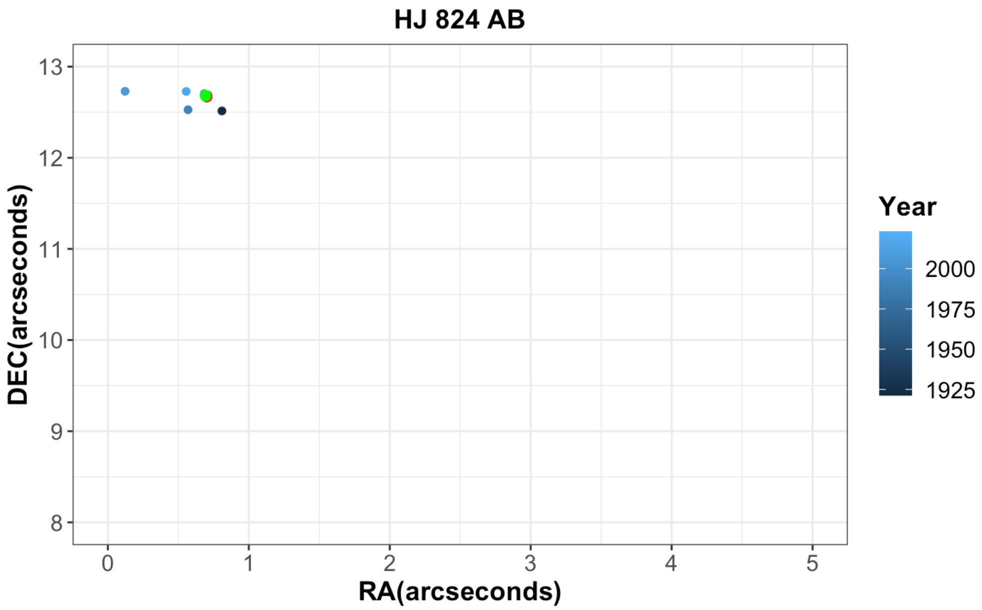

Figure 5: Position Plot of HJ 824's Secondary Star Over Time

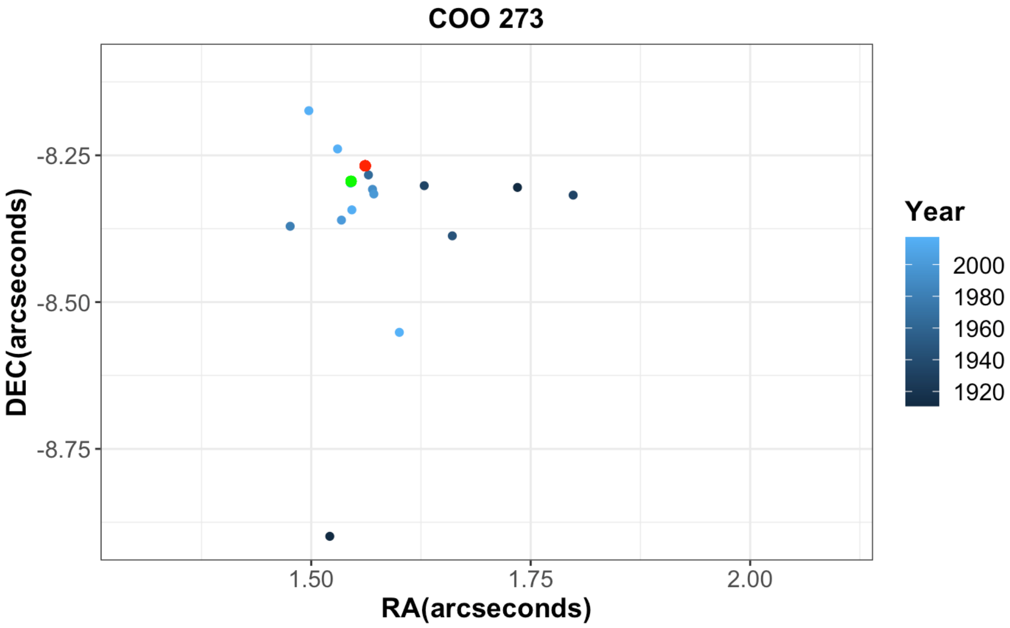

Figure 6: Position Plot of COO 273's Secondary Star Over Time

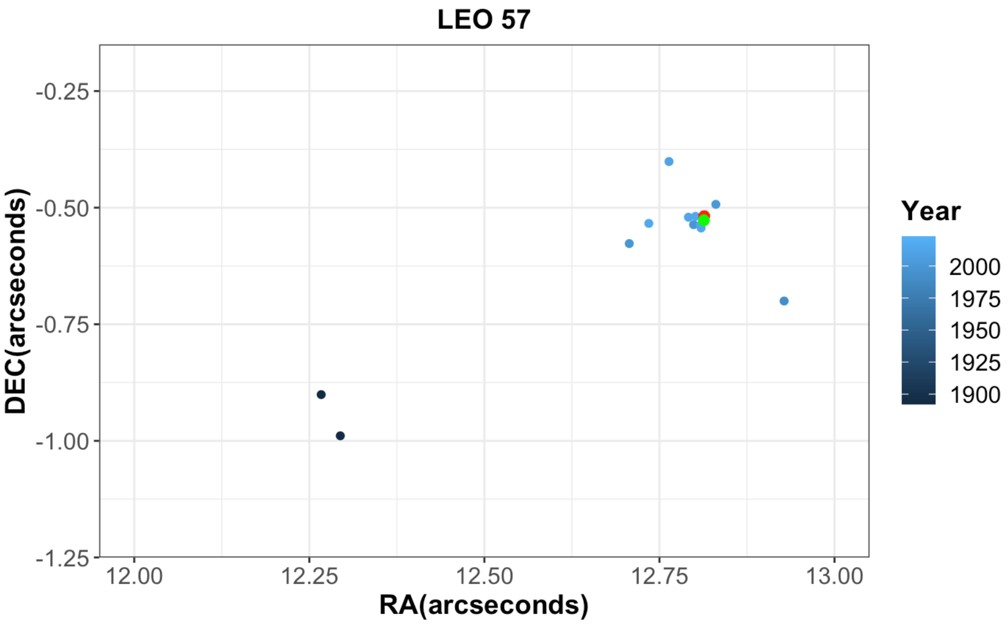

Figure 7: Position Plot of LEO 57's Secondary Star Over Time

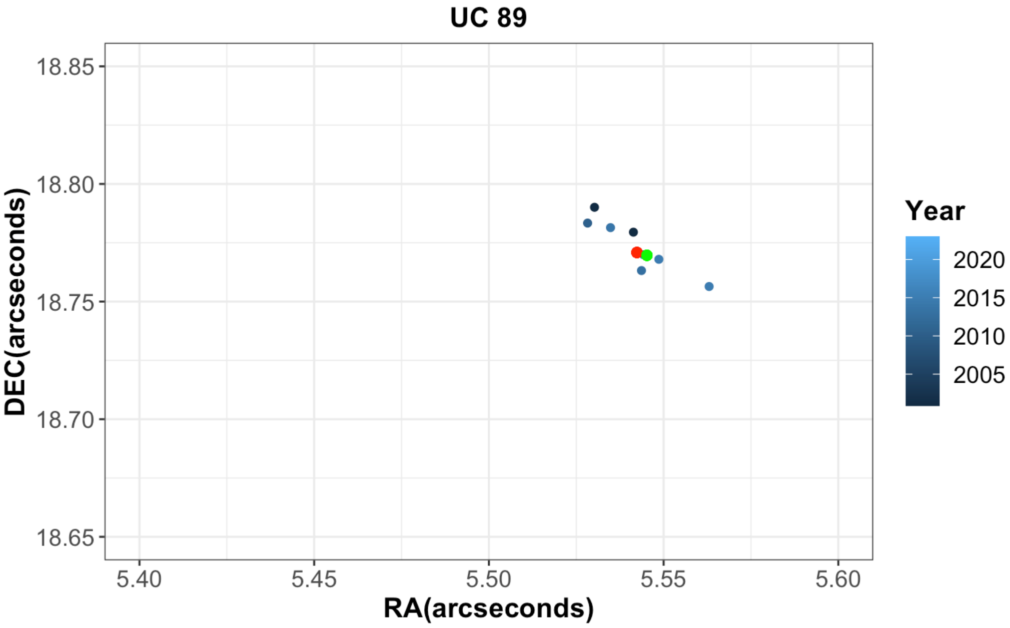

Figure 8: Position Plot of UC 89's Secondary Star Over Time

The plots of Figs. 5-8 provide a second way of analyzing the system over time. If the secondary star is gravitationally bound to the primary and has a reasonable period, some evidence of motion about the origin would have been evident within the plot of the secondary star position over time. Two of the stars display this arc-like motion, UC 89 and HJ 824. It is important to note, however, that accounting for the time of each data point as shown in the colormap, both stars seem to be moving back and forth along the arc of their motion. Although they have seemingly periodic motion, it is not likely that the stars are gravitationally bound as their motion does not form a continuous arc with their historical data. Two of the stars do not display any arc-like motion at all: COO 273 and LEO 57. For COO 273 and LEO 57, the star systems are likely not bound or have very long periods of several centuries or millennia if they are bound at all.

4. Discussion

In addition to comparing the Proper Motions of the stars, we also calculate the systems' relative velocity and determine the maximum spatial and radial separation these systems can have so that their relative velocity is less than the system escape velocity.

The transverse relative motion of the stars was calculated using the Proper Motion data in Table 3. In addition, Gaia also supplies the radial velocity of all eight stars studied. So the relative velocity can be calculated using the Pythagorean Theorem:

$$v_{relative} = \sqrt{(v_{radial})^2 + (v_{transverse})^2}$$

Table 4 presents these calculations.

Table 4: Relative velocities of all four systems.

System	Primary radial velocity (m/s)	Secondary radial velocity (m/s)	Relative radial velocity (m/s)	Relative transverse velocity (m/s)	Relative velocity (m/s)
HJ 824	12864	12104	760	2638	2746
COO 273	-3137	-3773	636	4894	4936
LEO 57	-5027	-5211	184	229	294
UC 89	823	479	344	1842	1874

We can find the masses of the stars in all four systems using either previous measurements or the stars' visual absolute magnitudes and their BP-RP differences found from the GAIA DR3. The primary of HJ 824 has been observed to be a G0 type star, with a mass of approximately 1.07 solar units (Cruzalèbes et al., 2019). An inference made from observational Hertzsprung-Russell (H-R) diagrams with Gaia magnitudes (Babusiaux et al., 2018) estimates the secondary to be also a G-type star with a mass of approximately 1 solar unit. Both stars in the system LEO 57 have a mass of around 2.3 solar masses, as found by Jiménes-Esteban et al (Jiménez-Esteban et al., 2019). Again using observational H-R diagrams, COO 273's primary and secondary were also estimated to be either Type G or Type F stars with masses of around 1.2 solar units. Using the same method, the primary of UC 89 was estimated to be around 1.1 solar masses, while the secondary was estimated to be around 0.8 solar masses. These mass estimations are presented in Table 5.

The escape velocity of a double star system is given by

$$v_{escape} = \sqrt{\frac{2G(m_{primary} + m_{secondary})}{r}}$$

where G is the gravitational constant and r is the separation of the stars in space. Thus, we can calculate the maximum spatial separation of the stars if they are bound:

$$r_{max} = \frac{2G(m_{primary} + m_{secondary})}{(v_{relative})^2}$$

We then calculate the transverse separation using the data from Gaia, and from this, we can calculate the maximum radial separation using the Pythagorean Theorem. These calculations are presented in Table 5. Note that sometimes the maximum spatial separation r_{max} is smaller than the transverse separation, in which case the stars are very likely not gravitationally bound. For these cases, we will write "N/A" for the maximum radial separation.

Table 5: Mass estimations and calculated maximum spatial and radial separation.

System	Primary mass (solar masses)	Secondary mass (solar masses)	Maximum spatial separation (AU)	Transverse separation (AU)	Maximum radial separation (AU)
HJ 824	1.07	1	495	2846	N/A
COO 273	1.2	1.2	165	2537	N/A
LEO 57	2.33	2.30	95300	14851	94080
UC 89	1.1	0.8	969	4620	N/A

From the above table, we can see that the three systems other than LEO 57 are all unlikely to be bound. LEO 57, on the other hand, has a possibility of being bound as the uncertainty range of the parallaxes for the primary and secondary overlap, so there is a good chance that the radial separation is less than the 94000 AU required for the system to be bound.

5. Conclusions

Measurements of four double star systems (HJ 824, COO 273, LEO 57, and UC 89) with similar parallax and proper motions were taken from images from the Las Cumbres Observatory, then compared to previous measurements. These data closely matched data of these stars from the Gaia Data Release 3. Additional Gaia data was also used to determine the relative velocity of the stars and estimate their masses. The maximum spatial and radial separation was calculated by setting the escape velocity equal to the relative velocity. The results suggest that three of the four systems (HJ 824, COO 273, and UC 89) are unlikely to be gravitationally bound, though they do have similar proper motion that suggests a shared history. However, the parallax uncertainties of the stars of LEO 57 overlapped, and calculations showed that if the radial separation of the two stars is less than 94000 AU, then they have a chance of being bound.

Acknowledgements

This research was made possible by the Washington Double Star catalog maintained by the U.S. Naval Observatory, the Stelledoppie catalog maintained by Gianluca Sordiglioni, Astrometry.net, and AstroImageJ software which was written by Karen Collins and John Kielkopf.

This work has also made use of data from the European Space Agency (ESA) mission Gaia (https://www.cosmos.esa.int/gaia), processed by the Gaia Data Processing and Analysis Consortium (DPAC, https://www.cosmos.esa.int/web/gaia/dpac/consortium). Funding for the DPAC has been provided by national institutions, in particular the institutions participating in the Gaia Multilateral Agreement.

This work makes use of observations taken by the 0.4m telescopes of the Las Cumbres Observatory Global Telescope Network located at the Siding Spring Observatory in Australia, at the Cerro Tololo Observatory in Chile, and at the Tenerife Observatory in Spain.

The authors would like to thank Richard Harshaw for his review of this work.

References

Cruzalèbes, P. et al. (2019). A catalogue of stellar diameters and fluxes for mid-infrared interferometry, Monthly Notices of the Royal Astronomical Society, 490(3), 3158–3176. https://doi.org/10.1093/mnras/stz2803

Gaia Collaboration, C. Babusiaux, F. Van Leeuwen, et al. (2018). Gaia Data Release 2: Observational Hertzsprung-Russell diagrams. A&A 616, A10. https://www.aanda.org/articles/aa/full_html/2018/08/aa32843-18/aa32843-18.html

Gaia Collaboration, T. Prusti, J.H.J. de Bruijne, et al. (2016b). The Gaia mission. A&A 595, A1. https://www.aanda.org/articles/aa/full_html/2016/11/aa29272-16/aa29272-16.html

Gaia Collaboration, A. Vallenari, A. G. A. Brown, et al. (2022k). Gaia Data Release 3: Summary of the content and survey properties. arXiv e-prints, https://arxiv.org/abs/2208.00211

Harshaw, Richard (2016). CCD Measurements of 141 Proper Motion Stars: The Autumn 2015 Observing Program at the Brilliant Sky Observatory, Part 3. Journal of Double Star Observations, 12(4), 394–399. http://www.jdso.org/volume12/number4/Harshaw_394_399.pdf

Jiménez-Esteban, F. M., E. Solano, and C. Rodrigo. (2019). A Catalog of Wide Binary and Multiple Systems of Bright Stars from Gaia-DR2 and the Virtual Observatory. The Astronomical Journal. 157(2):78, 1–10.https://iopscience.iop.org/article/10.3847/1538-3881/aafacc/pdf